

Stratospheric Variability in Summer

DAVID RIND

*Goddard Institute for Space Studies, New York, NY 10025 and Lamont-Doherty Geological Observatory,
Columbia University, Palisades, NY 10964*

WILLIAM L. DONN

Lamont-Doherty Geological Observatory, Columbia University, Palisades, NY 10964

W. ROBINSON

Columbia University, New York, NY 10027

(Manuscript received 18 October 1979, in final form 21 January 1981)

ABSTRACT

Rocketsonde observations and infrasound results are used to investigate the variability of the summer stratopause region during one month in summer. It is found that fluctuations of 2–3 days and about 16-day periods are evident, which appear to be vertically propagating. In this month the 2–3 day oscillations have an amplitude envelope equal in period to the longer period oscillations, implying a connection between the two phenomena. Observations of the diurnal tide and shorter period variability during the month are also presented.

1. Introduction

During the summer of 1977, as part of a program to determine the variability of the stratosphere, rocketsonde measurements of various parameters once a day for one month (11 July–10 August) were made at Wallops Island. Infrasound observations at Palisades, New York, were analyzed for this time period. Infrasound results during summer at this location can be used to determine the sound velocity near the stratopause (Rind *et al.*, 1973) and have been used to gauge the variability during stratospheric warmings (Rind and Donn, 1978). In this paper we compare results from these two different techniques and report on the variability observable with continuous measurements.

2. Infrasound technique

Infrasound between 0.1 and 1 Hz is generated by interfering ocean waves (Posmentier, 1968; Donn and Naini, 1973) and propagates with a vertical component until it reaches a level in the atmosphere where the ambient sound velocity in the direction of propagation exceeds the surface level value. It then refracts back to the surface, with its horizontal trace velocity equaling the sound velocity at this

upper "reflection" level (Rind *et al.*, 1973). For ocean wave sources to the east of Palisades this level will occur in regions of east winds and relatively high temperatures—the thermosphere in winter (Donn and Rind, 1972; Rind, 1978) and the stratosphere in summer and during stratospheric warmings (Rind *et al.*, 1973; Rind and Donn, 1978). The infrasound is recorded by surface level microphones and analyzed to determine the horizontal trace velocity; as infrasound is generated and recorded continuously, observations of upper level sound velocities are possible throughout the day. A short discussion of minor uncertainties in relating infrasound variations to wind variations is given in the Appendix.

Infrasound observations were made as a matter of routine during the summer of 1977 and analyzed for the interval which coincides with the Wallops Island observations. The results were compiled by averaging over an entire hour, and were determined for every other hour during the month of 11 July–10 August 1977. This should be contrasted with the rocketsonde observations at Wallops Island which reported instantaneous results once a day. Furthermore, Wallops Island is located some 350 km to the south of Palisades. Despite these temporal and spatial differences, a good comparison was achieved, as described below.

3. Comparison of rocketsonde and infrasound observations

Infrasound is reflected from regions with relatively high temperature and with winds from the direction of the source; as sound sources to the east are most common for our station, easterly winds favor such reflection.

During summer, the stratospheric circulation is controlled by the polar anticyclone, formed due to solar radiation absorption. The circulation around this feature provides easterly winds from ~20–80 km. Because the warmest temperatures occur in the vicinity of 50 km, we decided to compare the infrasound sound velocities with the Wallops Island sound velocities at various levels near this stratopause. The level with the best comparison is the one most responsible for infrasound reflection and the one which is being best “observed” with infrasound recording.

TABLE 1. Mean difference between the infrasound (IS) velocity and rocketsonde velocity at various layers; also the cross-correlation coefficient between the data sets at -1, 0 and +1 day lags.

Elevation (km)	$\Sigma OBS - IS $ (m s ⁻¹)	-1 day lag	0 day lag	+1 day lag
40–45	18.5	0.21	0.30	0.10
45–50	8.6	0.16	0.52	0.48
50–55	9.5	0.17	0.48	0.61
55–60	8.5	0.13	0.01	0.37
peak 45–50	6.3	0.07	0.50	0.49

In particular, we determined the sound velocity from the horizontal trace velocity of the observed infrasound and compared it with the average sound velocity (a function of both wind and temperature) determined at Wallops Island between 40–45, 45–50, 50–55 and 55–60 km, as well as the peak (highest) sound velocity between 45 and 50 km. During

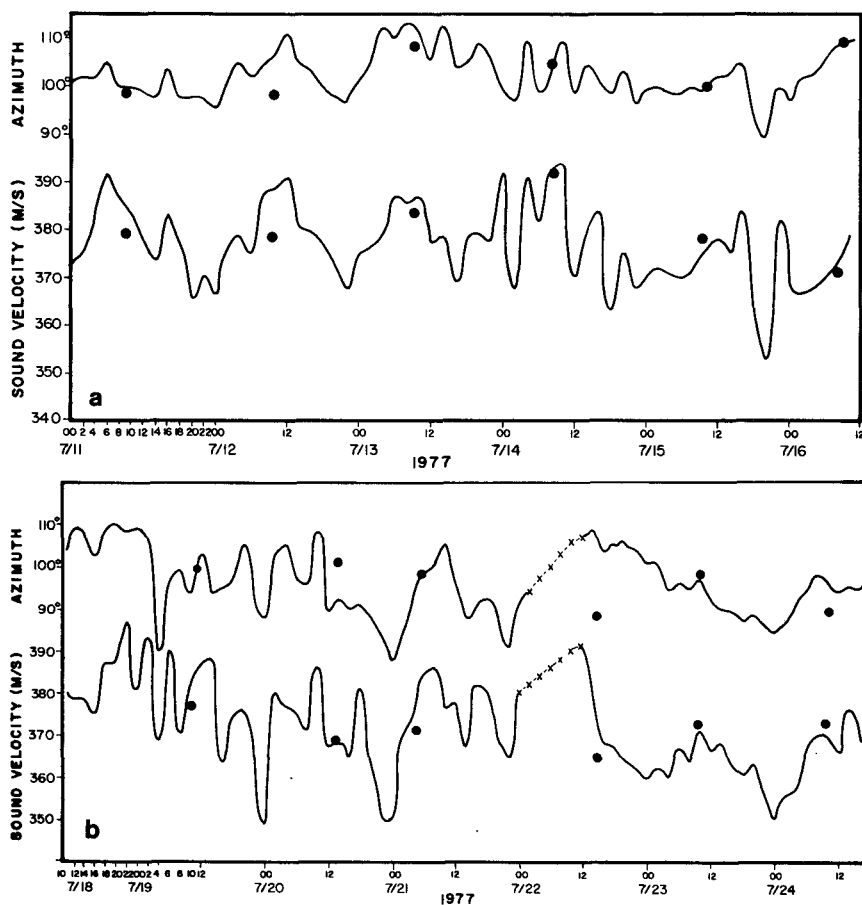


FIG. 1. Infrasound horizontal trace-velocity and azimuth at Palisades, New York, for the period 11 July–11 August 1977. Values averaged over an hour are plotted for every second hour (EST). Data with low confidence are indicated by broken lines, otherwise the velocities have an uncertainty of ± 2 m s⁻¹, and an azimuth of $\pm 2^\circ$. Also, shown are the rocketsonde peak sound velocities for the 45–50 km region (filled circles) recorded at Wallops Island, 300 km to the south.

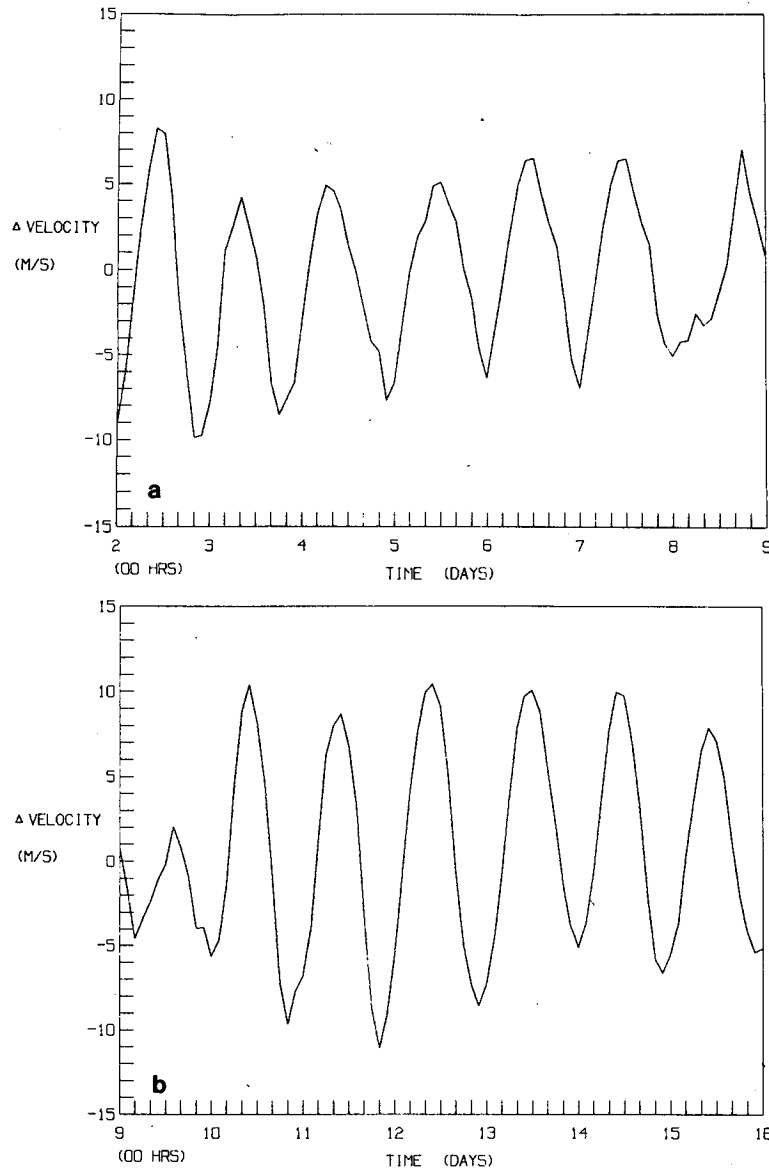


FIG. 2. 24 h (tidal) oscillation in sound velocity extracted with a 21-point filter.

the summer, there are few discrete ocean wave sources; rather the general area to the east of Palisades acts as an infrasound generator. It thus seemed possible to observe azimuthal variations associated with the changing meridional component of the wind, hence we compared the azimuth of the recorded infrasound with the azimuth of the wind velocity at the level of peak sound velocity between 45 and 50 km. (To do this for the Wallops Island observations, we added the magnitude of the observed wind to the scalar sound speed from temperature to get the total sound velocity, and noted the azimuth of the wind.)

The comparison of the sound velocities is presented in Table 1. We first compared the absolute

value of the difference between the rocketsonde observation at the various levels and the infrasound results for the nearest hour. The difference was relatively uniform between 45 and 60 km; however, the best comparison was with the peak value between 45 and 50 km. We then calculated the cross correlation between the two data sets. With the *a priori* assumption of 0 day lag null hypothesis the infrasound correlation with the observed data in the 45–50 km region is significant at the 1% level. The correlation falls off rapidly above 55 km and below 45 km. Thus, we will take the infrasound data to be representative of the 45–50 km (peak) sound velocity. The correlation of 0.5 accounts for only 25% of the variance, a point which we will return to later.

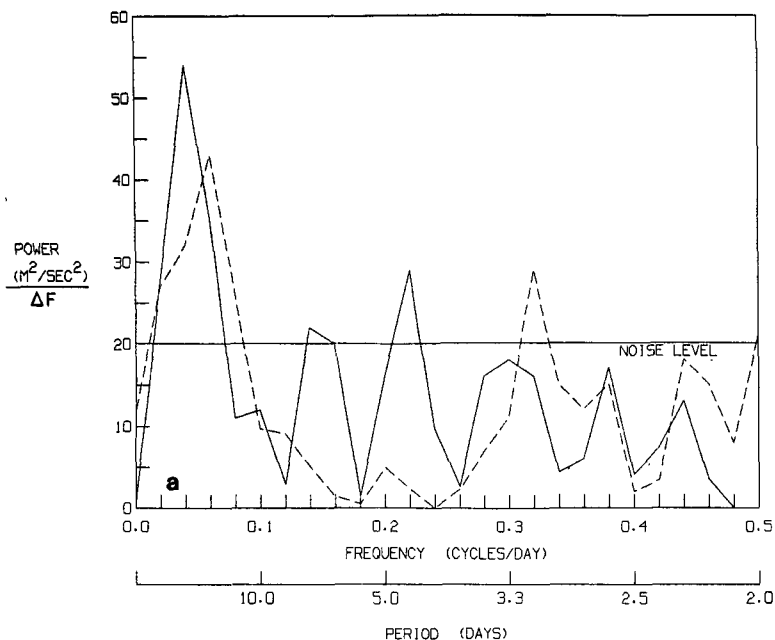


FIG. 3a. Simple periodogram estimate of the power spectra of the infrasound (solid line) and 45-50 km peak rocketsonde (dashed line) sound velocities. The noise level represents the 95% confidence level. $\Delta f = 0.02$ cpd.

Also shown in Table 1 are the correlations at -1 and $+1$ day lags. Above 50 km the correlations are higher at $+1$ day lag than with no lag; this is especially true for the region 55-60 km. Below 45 km the correlations, although low, favor the 0 to -1

day lag. If the correlations are caused by waves propagating vertically with a phase speed of 5 km day^{-1} (e.g., Perry, 1967), then the results are understandable. The waves which appear in the infrasound data, representing the 45-50 km region,

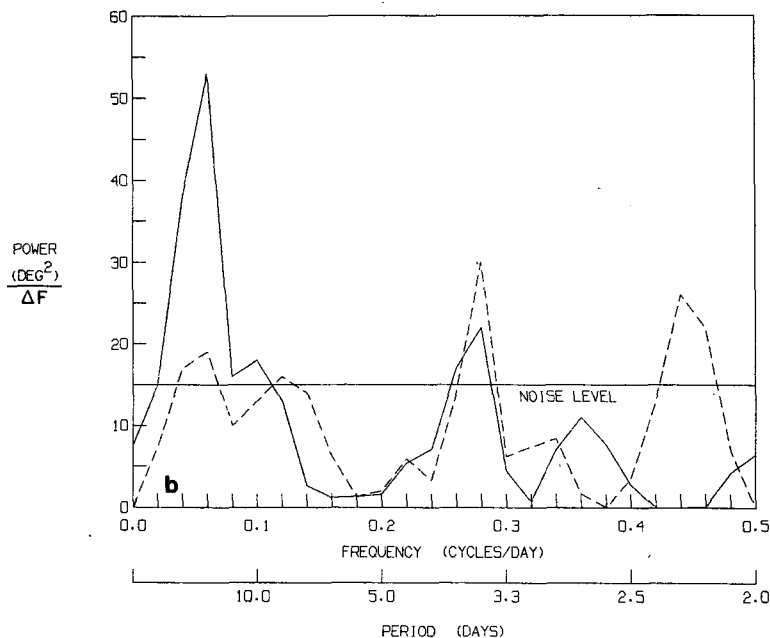


FIG. 3b. As in Fig. 3a for azimuthal fluctuations.

would appear below 45 km one day earlier, and at 55 km one day later. This will be discussed further, below.

4. Spectra

The infrasound results calculated for every other hour for a portion of the period 11 July–10 August are shown in Figs. 1a and 1b along with the peak sound velocity and azimuth for the 45–50 km region. The mean difference in the wind velocities determined by the two techniques was $6.7 (\pm 5)$ m s^{-1} while the azimuthal difference was $4.8 (\pm 6)$ deg. Given the apparent fluctuating nature of the stratospheric sound velocities, these differences could be accounted for by the lack of space and time coincidence between the two data sets. In both types of observations the sound velocity varied between 365 and 395 m s^{-1} , and the azimuth varied from $80\text{--}110^\circ$.

Figs. 2a and 2b show a portion of the filtered 24 h sound velocities; they indicate a peak-to-peak amplitude of 13 ± 3 m s^{-1} , with minimum sound velocity from the east at 2300 ± 2.7 h. This is in agreement with the observed phase of the diurnal tidal wind near the summer stratopause (Nastrom and Belmont, 1976). To investigate the energy spectrum for the longer periods, periodogram estimates of the power spectra of the two data sets (the infrasound observations and the 45–50 peak values) were

calculated for both the sound velocities and directions and are shown in Figs. 3a and 3b. The white-noise level was determined using a Fisher's test (Nowroozi, 1967) with 95% confidence. In Fig. 3a, significant peaks appear centered near the 3- and 15-day periods in the rocketsonde data, and near 4–5 days and 25 days in the infrasound data. In Fig. 3b, both data sets indicate significant energy centered at 3.5 and 15 days. Using the two data sets the cross-spectral peaks of the sound velocities (Fig. 4) are significant in the 2–3 day range and also at periods longer than 14 days, which is confirmed by the cross spectra of the azimuths (not shown). However, given the short length of the data sample relative to the longer period signal, it is obviously not possible to observe many oscillations of the phenomenon.

To look at these two period ranges in more detail, the sound velocities and azimuths were filtered with a low-pass filter (high-frequency cutoff at 6-day period). The results are shown (as deviations from the mean) in Figs. 5a and 5b. The long-period sound velocity variations are highly correlated (0.9). Both the sound velocities and the azimuths show little phase lag in the data sets, in agreement with the conclusion drawn earlier that the infrasound observations refer to the 45–50 km region. In comparison, the low-pass filtered infrasound velocities and the observed sound velocities for the 55–60 km region have a phase lag of about three days, with a correlation of 0.85. Apparently the long period

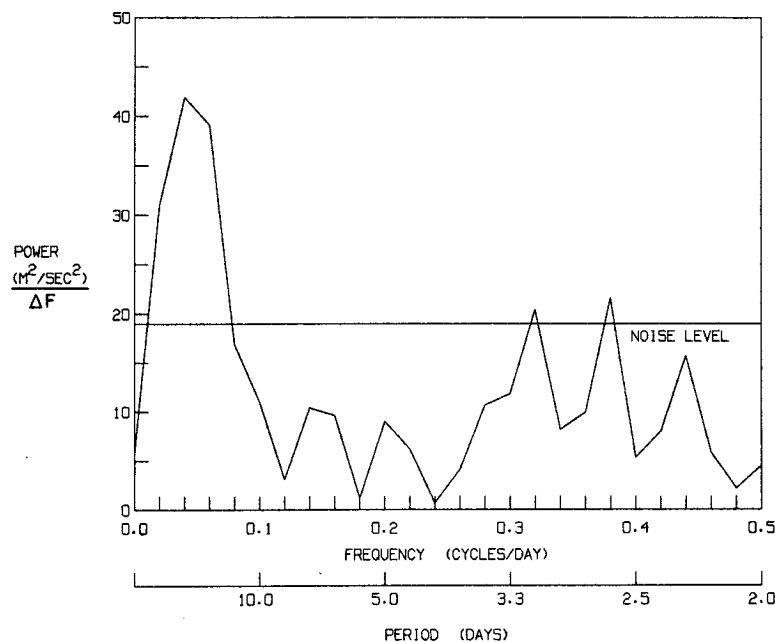


FIG. 4. Magnitude of cross spectra of the two data sets, with the 95% confidence level; Δf equals 0.02 cpd. Noise level determined as in Fig. 3.

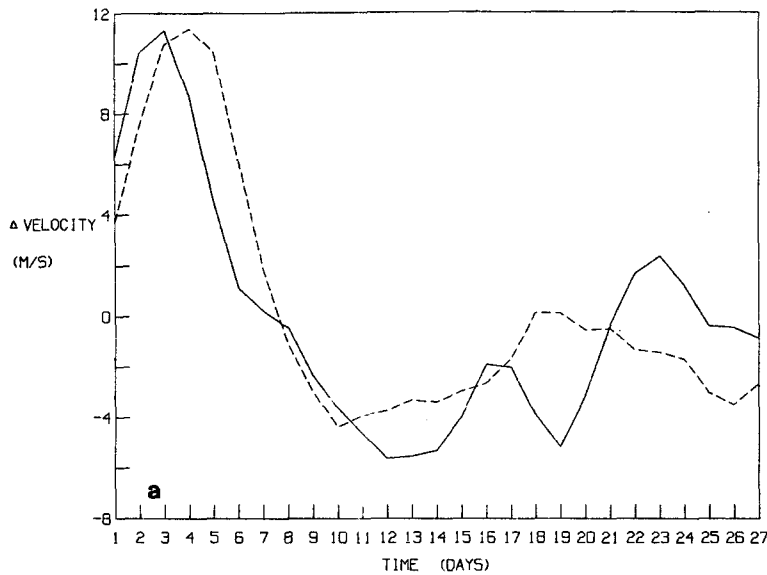


FIG. 5a. Low-pass filtered (6-day cutoff) sound velocity deviations for infrasound (solid line) and 45-50 km peak rocketsonde (dashed line) observations.

waves, which appear in the spectra for all the levels, do represent a vertically propagating phenomenon.

The 2-3 day high-pass filtered sound velocities are shown in Fig. 6 for the infrasound and the 45-50 km region. A striking in-phase relationship can be seen when the amplitudes are large, with little relationship when the amplitudes are low. Again, no phase lag is apparent. Note also what appears to be a longer period envelope in the amplitude. In contrast, when the infrasound is compared with the

55-60 km sound velocities, an apparent phase lag of about seven days exists (with a correlation of 0.7), again an indication of vertical propagation, although twice as slow as for the longer period waves. In contrast to the longer period waves, these waves are only weakly evident at 40-45 km, implying their generation may be connected with the stratospheric jet. The larger period amplitude envelope (with a period of ~16 days) implies their generation may be connected with the longer period waves.

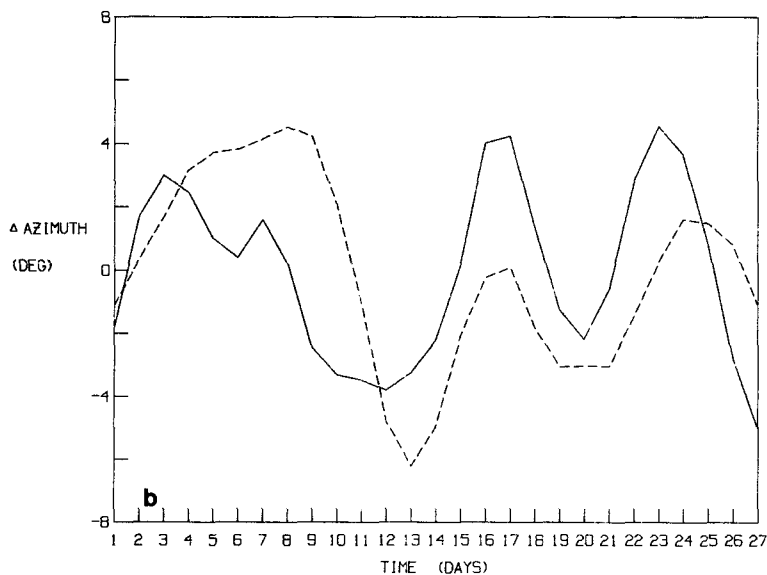


FIG. 5b. As in Fig. 5a except for azimuths.

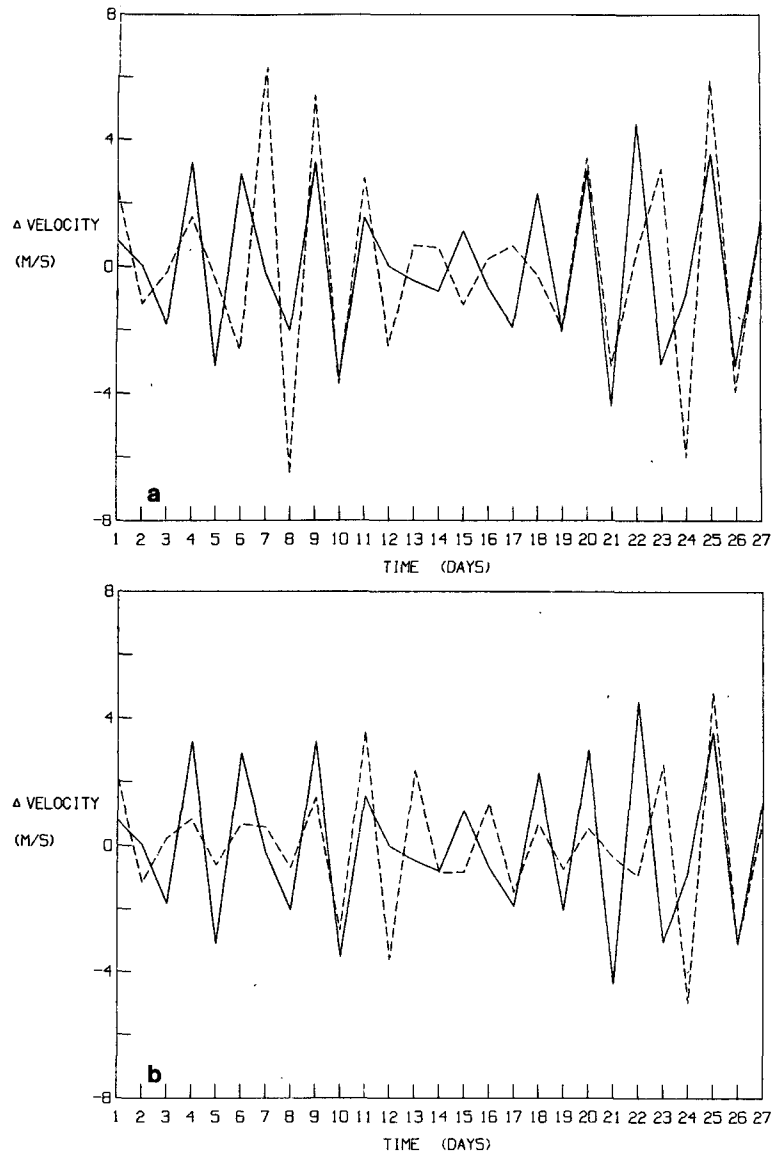


FIG. 6 As in Fig. 5a except for high-pass (2–3 days) sound velocities.

The availability of the infrasound data at 2 h periods allows the power spectrum for the month to be obtained with more confidence, and also provides a look at higher frequencies. A smoothed periodogram estimate of the power spectrum is shown in Figs. 7a and 7b for the sound velocities and azimuths. The white-noise level is calculated as before. Both show significant peaks at around 3- and 16-day periods. In Fig. 7a, the spectrum is compared to a “red-noise” level, generated by a first-order linear Markov process (e.g., Gilman *et al.*, 1963), using the one-lag value of the autocorrelation; the significance remains unaffected. In addition, in order to investigate the longer period part of the spectrum, the data was subjected to a maximum entropy analysis (MEM) known to pro-

vide more sensitive determinations of spectra when the data sample is not long compared to the period of waves with significant energy (e.g., Ulrych, 1972). The frequencies of the short-period and long-period peaks remained unchanged.

Fig. 7 also indicates the presence of a diurnal (tidal) oscillation which, as noted previously, agrees with the observed diurnal tide near the summer stratopause. There is no evidence of a semidiurnal oscillation, which is known to be small at these heights (e.g., Beyers *et al.*, 1966).

5. Short-period variability

Fig. 1 indicates the degree of variability apparent near the stratopause in summer. The mean variability between observations 2 h apart (with the

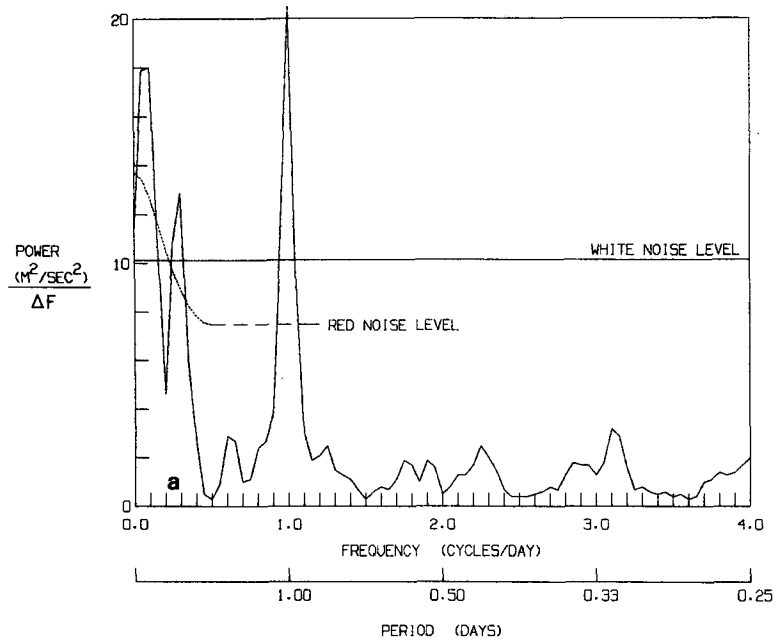


FIG. 7a. Power spectra for 2 h data infrasound velocities. The white noise level is the 95% confidence level. The red-noise level is derived from the 1-day lag autocorrelation value with the diurnal cycle removed. The bandwidth Δf is 0.05 cpd.

observations averaged over the entire hour) is 6 m s^{-1} . This can be compared with observations of zonal wind velocity variability at 45–50 km on the order of 2 h from rocketsonde data at White Sands and the Atlantic Missile Range (Lowenthal, 1966). For 50 different soundings, the 2 h variabil-

ity for all seasons was 7 m s^{-1} in good agreement with the infrasound result (despite inclusion of rocketsonde soundings from all seasons and despite the use of instantaneous data). We also can compare these results with gravity wave and traveling planetary wave effects for all seasons determined

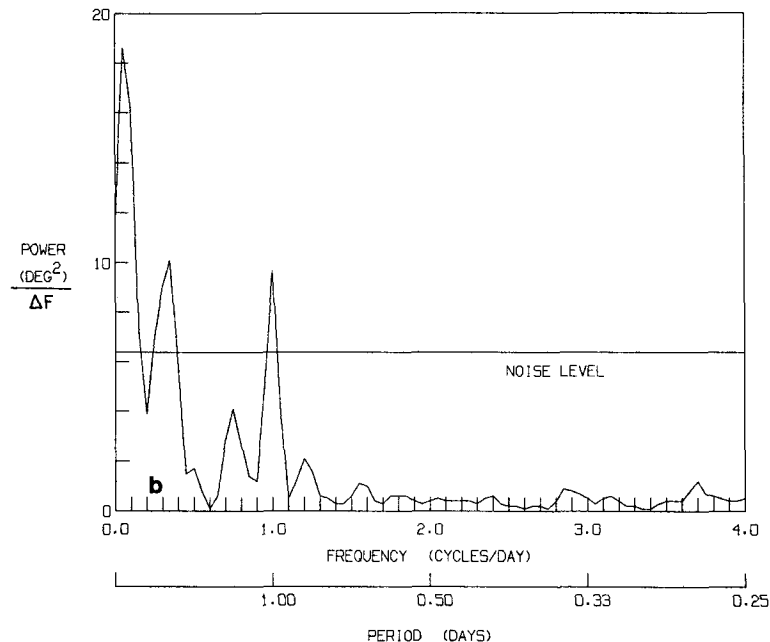


FIG. 7b. As in Fig. 7a except for azimuthal variations.

from various data sites (Justus and Woodrum, 1973). In the 45–65 km region, 0–2 h gravity wave perturbations in the zonal wind averaged close to 7 m s^{-1} , again, in good agreement with the infrasound results. The short-period oscillations (perhaps gravity waves) responsible for these variations are not coherent over long averaging periods and thus do not appear on spectra averaged over an entire month; nevertheless, they appear to possess appreciable amounts of energy.

6. Discussion

Both the infrasound and rocket data indicate significant energy with fluctuations on the order of 5 m s^{-1} in the period range of 2–3 days and around 16 days. Waves with periods of 10–20 days are often seen in satellite radiance data (e.g., Quiroz, 1975) associated with traveling planetary waves in winter. Although the east wind regime in the summer stratosphere acts to reflect waves propagating from the troposphere, waves which move westward have a better chance of propagating vertically. Thus, transient waves have been observed to be of equal or greater importance compared with stationary waves in the NH summer stratosphere (McNulty, 1976; Hirota, 1976). The phase speeds of the observed westward traveling waves (of wavenumber 1 or 2) varied, and thus the observed periods range from as high as 10–30 days (Deland, 1973; Hirota, 1976) to 3 days (Deland, 1973). These observations imply that the long-period fluctuations we observe may be due to traveling planetary waves, although with only one observing station we cannot determine the horizontal wavelength or phase velocity of these perturbations.

Waves of about 2-day period have often been observed in the mesosphere (e.g., Kingsley *et al.*, 1978). The data here imply that waves of 2–3 day period are propagating vertically in the stratopause region, that their energy may be weaker below 45 km, and that their amplitude, at least for this month, has an envelope whose period is similar to that of the observed longer period waves. This leads to the speculation that the waves are being generated in the stratopause region in conjunction with the vertical propagation of the longer period waves. An alternate explanation would be to associate the 2–3 day and 16-day oscillations with free oscillations (e.g., Salby and Roper, 1980). In this case, the fluctuations would be generated by random perturbations, and the periods would represent preferred time scales of oscillation. The energy would not propagate vertically. Although this contrasts with the apparent phase lags noted here between the various levels, more observations of both the vertical and horizontal structure are necessary before any identification can be made with confidence.

Acknowledgments. This research was supported by the Atmospheric Sciences Research Section of the National Science Foundation under Grant ATM 08350 and U.S. Army Research Office under Grant DAAG 0131. We also would like to thank Frank Schmidlin at Wallops Island for kindly furnishing us with the rocketsonde observations.

APPENDIX

Infrasound and Wind Variations

It is important to note that the sound velocity data are not obtained at a constant azimuth (e.g., Fig. 1); this lowers the amplitude of the observed fluctuations as the azimuth to some extent follows the maximum velocity. However, the azimuthal variations are not excessive, so this can reduce the total amplitude by only a small amount. For example, if the observed wind speed from the northeast were 60 m s^{-1} (composed of 45 m s^{-1} prevailing wind and a diurnal tidal amplitude of 15 m s^{-1} directed at this hour to the southwest), 12 h later one would expect to observe a wind speed of 30 m s^{-1} (45 m s^{-1} prevailing— 15 m s^{-1} tidal) from the northeast. If, however, the observed sound velocity azimuth also changes by, say, 20° (e.g., Fig. 1) to a more easterly direction, the tidal velocity effect on this new direction is only 14 m s^{-1} , with an observed wind velocity now of 31 m s^{-1} . The net reduction in the 'observed' tide is then $<1 \text{ m s}^{-1}$.

Another cautionary note is that sound velocity variations can be caused by both temperature and wind fluctuations. Due to dependence of sound velocity on the square root of temperature, temperature fluctuations of the same magnitude as wind fluctuations will be less important, and hence have not been emphasized here—however, observations of the tidal temperature range at the stratopause (e.g., Beyers *et al.*, 1966) indicate the possibility of sound velocity changes of several meters per second from this effect alone.

REFERENCES

- Beyers, N., B. Miers and R. Reed, 1966: Diurnal tidal motions near the stratopause during 48 hours at White Sands Missile Range. *J. Atmos. Sci.*, **23**, 325–333.
- Deland, R., 1973: Analysis of Nimbus 3 SIRS radiance data: Traveling planetary-scale waves in the stratospheric temperature field. *Mon. Wea. Rev.*, **101**, 132–145.
- Donn, W., and D. Rind, 1972: Microbaroms and the temperature and wind of the upper atmosphere. *J. Atmos. Sci.*, **29**, 156–172.
- , and B. Naini, 1973: Sea wave origin of microbaroms and microseisms. *J. Geophys. Res.*, **78**, 4482–4488.
- Gilman, D., F. Fuglister and J. Mitchell, Jr., 1963: On the power spectrum of red noise. *J. Atmos. Sci.*, **20**, 182–184.
- Hirota, I., 1976: Seasonal variation of planetary waves in the

- stratosphere observed by the Nimbus 5 SCR. *Quart. J. Roy. Meteor. Soc.*, **103**, 757-770.
- Justus, C., and A. Woodrum, 1973: Upper atmospheric planetary-wave and gravity-wave observations. *J. Atmos. Sci.*, **30**, 1267-1275.
- Kingsley, S., H. Muller, L. Nelson and A. Scholefield, 1978: Meteor winds over Sheffield. *J. Atmos. Terr. Phys.*, **40**, 917-922.
- Lowenthal, M., 1966: Variability of rocket-measured winds. Tech. Rep. ECOM-2693, U.S. Army Electronics Command, Fort Monmouth, NJ, 21 pp. [NTIS #AO-632-597].
- McNulty, R., 1976: Vertical energy flux in planetary-scale waves: Observational results. *J. Atmos. Sci.*, **33**, 1172-1183.
- Nastrom, G., and A. Belmont, 1976: Diurnal stratospheric tide in meridional wind, 30 to 60 km, by season. *J. Atmos. Sci.*, **33**, 315-320.
- Nowroozi, A., 1967: Table for Fisher's test of significance in harmonic analysis. *Geophys. J. R. Astron. Soc.*, **23**, 517-520.
- Perry, J., 1967: Long-wave energy processes in the 1963 sudden stratospheric warming. *J. Atmos. Sci.*, **24**, 539-550.
- Posmentier, E., 1968: A theory of microbaroms. *Geophys. J. Roy. Astron. Soc.*, **13**, 487-501.
- Quiroz, R., 1975: The stratospheric evolution of sudden warmings in 1969-74 determined from measured infrared radiation fields. *J. Atmos. Sci.*, **32**, 211-224.
- Rind, D., 1978: Investigation of the lower thermosphere results of ten years of continuous observations with natural infrasound. *J. Atmos. Terr. Phys.*, **40**, 1199-1210.
- , and W. Donn, 1978: Infrasonic observations of variability during stratospheric warmings. *J. Atmos. Sci.*, **35**, 546-553.
- , ——— and E. Dede, 1973: Upper air wind speeds calculated from observations of natural infrasound. *J. Atmos. Sci.*, **30**, 1726-1729.
- Salby, M., and R. Roper, 1980: Long-period oscillations in the meteor region. *J. Atmos. Sci.*, **37**, 237-244.
- Ulrych, T., 1972: Maximum entropy power spectrum of truncated sinusoids. *J. Geophys. Res.*, **77**, 1396-1400.